Left-Ventricle Basal Region Constrained Parametric Mapping to Unitary Domain

Antoni Gurgui[1(✉)], Debora Gil[1,2], Vicente Grau[3], and Enric Marti[2]

[1] Computer Vision Center of Catalunya, Universitat Autonoma de Barcelona, Barcelona, Spain
agurgui@cvc.uab.cat
[2] Computer Sciences Department, Universitat Autonoma de Barcelona, Barcelona, Spain
[3] Department of Engineering Science, Institute of Biomedical Engineering, University of Oxford, Oxford, UK

Abstract. Due to its complex geometry, the basal ring is often omitted when putting different heart geometries into correspondence. In this paper, we present the first results on a new mapping of the left ventricle basal rings onto a normalized coordinate system using a fold-over free approach to the solution to the Laplacian. To guarantee correspondences between different basal rings, we imposed some internal constrained positions at anatomical landmarks in the normalized coordinate system. To prevent internal fold-overs, constraints are handled by cutting the volume into regions defined by anatomical features and mapping each piece of the volume separately. Initial results presented in this paper indicate that our method is able to handle internal constrains without introducing fold-overs and thus guarantees one-to-one mappings between different basal ring geometries.

Keywords: Laplacian · Constrained maps · Parameterization · Basal ring

1 Introduction

Building statistical models (or atlases) of the heart is central for investigating and understanding tissue functions and properties. A main step in this direction is the definition of reference frames, or unitary domains, that allow to compare different geometries in a meaningful way. Ideally, these domains should assign equal coordinates to corresponding anatomical features and, at the same time, align the intermediate zones that might present different shapes (i.e. different trabeculae architectures).

The definition of cardiac atlases is an active field of research and several methods to put the geometries into correspondence and build atlases have been proposed [13,19]. Existing methods can be split into two main categories. Methods that deform a geometry to another one [7,12] and those that build a parametric description of the ventricular shapes, using basis functions like thin-plate

T. Mansi et al. (Eds.): STACOM 2016, LNCS 10124, pp. 163–171, 2017.
DOI: 10.1007/978-3-319-52718-5_18

splines [2], hermite functions [11] or B-Splines [5], to define a mapping between different geometries. Recently, parameterizations using the solution to the Laplacian have been proposed to put cardiac surfaces into correspondence. In [14,16], a 3-step method to map the left ventricle cut at basal level onto a disk domain is proposed. A first unconstrained map is generated by solving the Laplacian with the boundary of the shape mapped to the boundary of the domain. Then, the apex is fixed to the center of the domain and a final parameterization if calculated using a quasi-conformal metric. Another example is presented in [10], where constraints for the atrial surface mapping are imposed by defining boundary conditions inside the domain.

However, most of the methods rely on a simplified geometry of the heart at the basal region, using a flat "top" and discarding the basal ring due to its complex shape. A main concern in cutting the geometry using a short axis plane to build cardiac models is the uncertainty of cutting possible connectivity of cardiac muscular architecture [15]. Although such connectivity has not been rigorously proved, several works [1,6] support the importance of fiber orientation in electromechanical simulations of the heart and, thus, we believe that basal connectivity should be explored. We propose to use the solution to Laplacian in order to define coordinates over the basal region of the left ventricle (LV). This enables to take this region into account when comparing different LV volumes. To this end, we propose to map the left ventricular basal structure to a normalized coordinate domain imposing some inner fixed positions on certain anatomical landmarks that are extended over the rest of the volume.

In this study we investigate the definition of a volumetric left ventricular base reference frame with constrained coordinates at some anatomical features, or places, based on the discrete mesh Laplacian presented in [17] and defining interior fixed coordinates as in [8]. This method presents the following advantages: allows to handle arbitrary polygonal constraints, can be extended to other organ geometries and it is easy to implement and reproduce.

2 Materials and Methods

To develop the method we have used the normal hearts from John Hopkins Canine Hearts database[1] [9]. This database consists of *ex-vivo* magnetic resonance image (MRI) volumes of canine hearts. More precisely, to focus on the basal ring, we studied the SA slices comprising the 35% (i.e. regions 1–6 of the AHA division [3]) of the left ventricle (LV) volume. We generated the initial volumetric meshes defining a vertex for each voxel and their connectivity from their 26-adjacency in the image.

To constrain interior coordinates, anatomical features and extracted geometric landmarks were fixed. Anatomical features include the basal ring, the endocardium and the epicardium. Geometric landmarks consist of medial surface of the volumes [18], the boundaries between interoseptal and inferoseptal and between inferolateral and anterolateral basal regions (see Fig. 1).

[1] Avaliable at: http://cvrgrid.org/data/ex-vivo.

2.1 Left Ventricle Volume Parameterization Using Laplacian Solution

Laplacian operators [4] are powerful mathematical tools that allow to define coordinate systems on manifolds, or volumes, with values fixed at some locations. These fixed values are called boundary conditions (BC) and can be coordinates constraints (Dirichlet BC) or derivative constraints (Neumann BC). When defining coordinate systems, Dirichlet conditions allow to constraint specific coordinates to specific locations, which are then extended by the solution of the Laplacian over the whole domain. This also implies that their setting is central to put different geometries into correspondence.

Given a 3D mesh $\mathcal{M}$ extracted from an MRI volume, we propose to obtain a parameterization from the Cartesian space to our defined 3D unitary domain $\mathcal{D} = [0,1] \times [0,1] \times [0.65,1]$ (see Fig. 1) using the 3 coordinate functions. We use a similar nomenclature as spherical coordinates and name our three unitary domain coordinates radius r for the depth coordinate ranging from endocardium to epicardium, angular θ for a circumferential coordinate defined in short axis (SA) and elevation φ for a coordinate defined in SA along the basal part of the left ventricles. Mathematically, we want to define a mapping between our mesh $\mathcal{M}$ to the unitary domain $\mathcal{D}$:

$$\begin{aligned} \mathbb{R}^3 \supset \mathcal{M} &\rightarrow \mathcal{D} \subset \mathbb{R}^3 \\ (x,y,z) &\rightarrow (r,\theta,\varphi) \end{aligned}$$

To obtain this mapping, we use the solution to the Laplacian to define each coordinate:

$$\left.\begin{array}{l} 1.\ \Delta r = 0 \text{ with } r|_{\mathcal{M}_r} = r_C \\ 2.\ \Delta\theta = 0 \text{ with } \theta|_{\mathcal{M}_\theta} = \theta_C \\ 3.\ \Delta\varphi = 0 \text{ with } \varphi|_{\mathcal{M}_\varphi} = \varphi_C \end{array}\right\} \tag{1}$$

for Δ the Laplacian operator, M_r, $\mathcal{M}_\theta$, $\mathcal{M}_\varphi$ the specific anatomical sites in the 3D mesh $\mathcal{M}$ where the values of each coordinate, r, θ, φ are constrained, respectively, to $r_C := r_C(x,y,z)$, $\theta_C = \theta_C(x,y,z)$ and $\varphi_C = \varphi_C(x,y,z)$.

As our domains are discrete meshes obtained from MRI volumes, we use the discrete Laplace operator to compute solutions to (1). By the mean value Theorem [4], solutions to Eq. (1) can be approximated by the following 3 linear systems (one for each coordinate):

$$1.\ Ar = b_R;\ \ 2.\ A\theta = b_\theta;\ \ 3.\ A\varphi = b_\varphi \tag{2}$$

with A a sparse matrix defined from the triangulation adjacency, the size of A being $N_v x N_v$ with N_v the number of mesh vertices [3] and b the independent term given by the boundary conditions evaluated at each anatomical site (M_r, $\mathcal{M}_\theta$, $\mathcal{M}_\varphi$). If $N(i)$ is the 1-ring of V_i defined as the n adjacent voxels in the volume, then A is given by:

$$A = \begin{cases} 1 & \text{if } j \in N(i),\ i \neq j \\ 0 & \text{if } j \notin N(i),\ i \neq j \\ -\sum_{k \neq i} a_{ik} & \text{if } i = j \end{cases} \tag{3}$$

Given that the matrix A is the same for the 3 coordinates and only depends on the mesh connectivity defined by the MRI volume, the only thing that remains to be defined are boundary conditions b_r, b_θ and b_φ and their corresponding anatomical meshes.

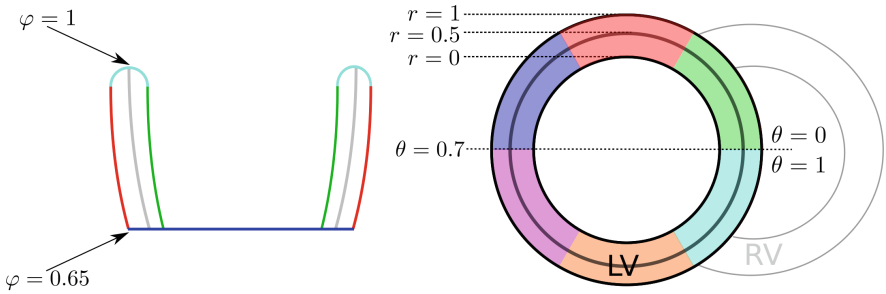

Fig. 1. Schematic description of fixed landmarks and their values in $\mathcal{D}$. Left: vertical long axis view, with the upper surface in light blue, the lowest plane in dark blue, the endocardium in green, the epicardium in red and the medial surface in grey. Right: SA view with colored AHA basal regions. (Color figure online)

2.2 Constrained Coordinates for the Left Ventricle

The fixed coordinates were defined using the following anatomical structures used by clinicians: the basal ring, the endocardium and the epicardium. The SA cut defining the lower boundary of the basal region was also considered to complete its boundary. Moreover, to demonstrate the capacity of the method to constrain interior boundaries, and have a better definition of the radial and elevation coordinates at the basal part, we have extracted the medial surface of each volume, as defined in [18]. In Fig. 2 we show these landmarks with respect to the volume. These anatomical landmarks are used to define boundary conditions for each coordinate as follows.

The values of some coordinates are well defined on some of the sites, like radius equal 0 at endocardium and equal 1 at epicardium. However, it is not so straightforward to extend such values to the complete basal region. We propose to use the Laplacian for surfaces to extend the values that are easily identified to the whole basal ring boundary (endocardium, epicardium, SA lower cut and basal region upper surface) to define the boundary functions for each coordinate. Such boundary functions will be used to obtain the coordinate value inside the whole volume solving each of the systems in (2).

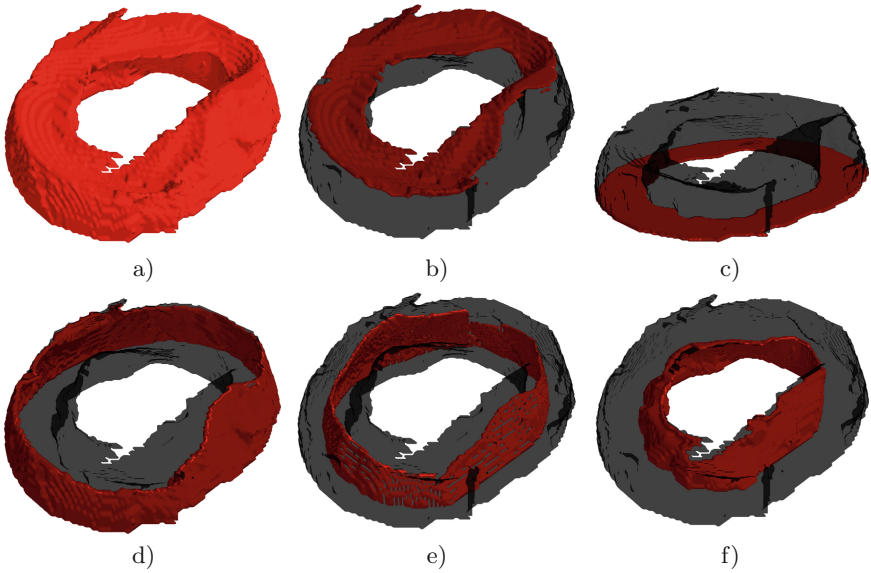

Fig. 2. Examples of segmentations masks: (a) whole volume, (b) upper surface, (c) lower plane, (d) epicardium, (e) medial surface and (f) endocardium

Radial Coordinate. The radial coordinate $r \in [0, 1]$ normalizes the width of the basal region and, thus, it should be set to $r = 0$ at the endocardium and $r = 1$ at the epicardium. To obtain a more accurate transition we force an additional interior constraint at the medial surface with $r = 0.5$. Therefore, the anatomical mesh $\mathcal{M}_r$ is given by endocardium, epicardium, basal ring, SA lower plane and the medial surface. The boundary function b_r is obtained from the values fixed at endocardium, epicardium and medial surface as follows.

We extend the radial coordinate over the basal ring upper surface and lowest SA plane of the volume ((Fig. 2b and c), respectively), using the solutions to the Laplacian for each surface (basal ring and SA cut). For each surface, the matrix A in (3) is computed using the connectivity given by their masks in the MRI volume. As boundary conditions, we set $r = 0$ in the intersection of each surface with the endocardium, $r = 0.5$ in the intersection with the medial surface and $r = 1$ in the intersection with the epicardium.

Angular Coordinate. The angular coordinate θ is the circumferential coordinate defined in SA along the volume, counterclockwise positive defined. This coordinate allows the unfolding of the LV as shown in Fig. 1. To define its origin $\theta = 0$ we have used the boundary between basal interoseptal and basal inferoseptal regions defined by the American Heart Association (AHA). At the same time, we have fixed $\theta = 0.7$ in the boundary between basal inferolateral and basal anterolateral regions. Although the "natural" coordinate value should be 0.5, we forced it to 0.7 to show the effect of fixing it.

Angular values defined at the surfaces separating the septal-lateral regions have to be extended to the whole anatomical site $\mathcal{M}_\theta$ to define b_θ. Since in this case $\mathcal{M}_\theta$ is given by the basal ring boundary, we independently solve the Laplacian for endocardium, epicardium, basal ring upper surface and SA lower plane with boundary conditions given by the intersection of the planes defining the septal and lateral regions with each of the 4 surfaces. The solutions to these Laplacians are used as boundary conditions in the second system of (2) to extend the angular coordinate to the whole volumetric mesh.

Elevation Coordinate. The elevation coordinate φ is defined in SA along the ventricular basal region and ranges from 0.65 at the lowest plane to 1 at the upper surface. These values are extended to $\mathcal{M}_\varphi$ given as before by the whole basal region boundary to define b_φ. To do so, we solve 2 Laplacian systems, one for the endocardium and another for the epicardium, with boundary conditions fixing their intersection with the basal ring to 1.0 and their intersection with the lower SA cut to 0.65. Finally, we propagate this elevation coordinate over the whole basal volume using these solutions to the Laplacian as boundary conditions in the 3rd system of (2).

3 Results

To illustrate the performance of the method, we have parameterized the ventricular basal region of 3 normal hearts from JHU canine cardiac database, labeled as DT080803, DT101703 and DT102403.

Figure 3 shows the 3 coordinate maps (r in 1st row, θ in 2nd row and φ in 3rd row) and the remeshing for the 3 cases in the last row. Remeshings show each coordinate isoline in a different color, red for r, green for θ and blue for φ. We observe that the propagation of each coordinate fixed at its specific anatomical site is smooth and homogeneous. This guarantees that the parametric map will be differentiable and will provide regular remeshings. The quality of the remeshing can be observed in the meshes of the last row, where we show the isolines of each coordinate map. It is worth noticing that their distribution over basal region is homogeneous in the 3 cases, which is a desirable property for a further use in cardiac models.

4 Discussion

The definition of reference frames, or unitary domains, that allow to compare different cardiac geometries in a meaningful way has several applications such as shape and function analysis or integration of data from different modalities. In this paper we have presented a method to obtain parameterizations of the left ventricle basal ring into a unitary domain. Moreover, with our method, we can go one step further and fix coordinate values in the unitary domain at anatomical features to force a more meaningful coordinate assignment.

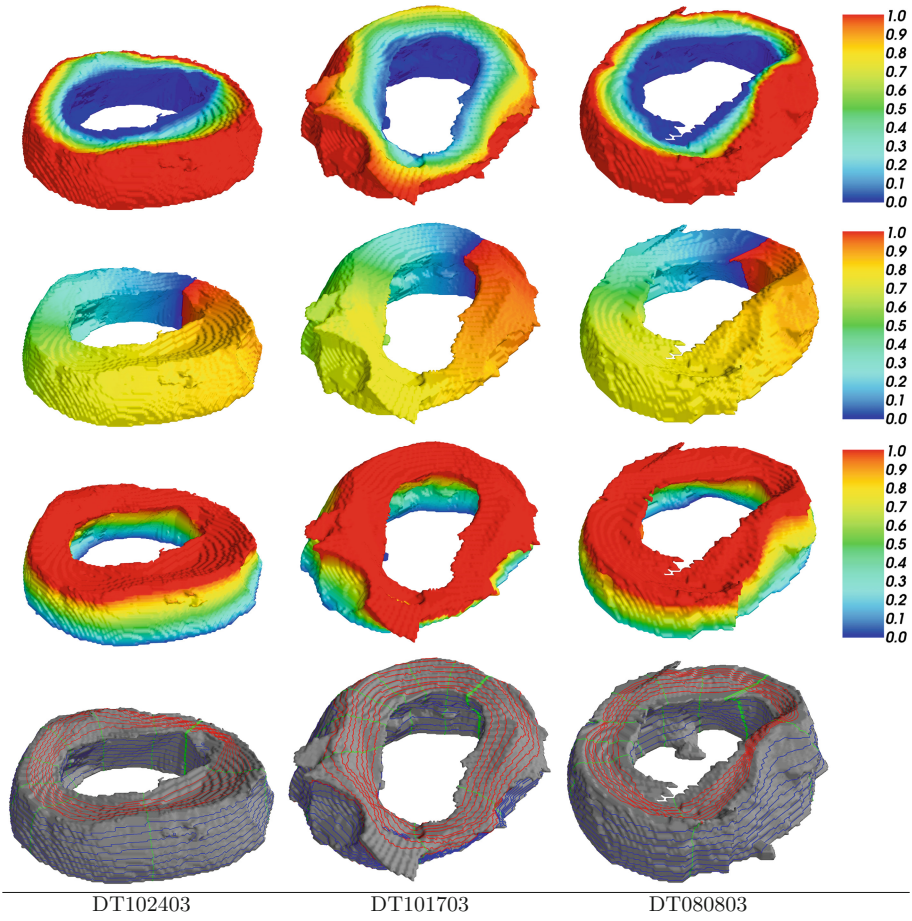

Fig. 3. Results of constrained coordinate extension. Top row: radial coordinate r. Second row: angular coordinate θ. Third row: elevation coordinate φ. Bottom row: isolines over the volume for each coordinate by color $(red, green, blue) = (r, \theta, \varphi)$ (Color figure online)

In order to be able to compare different anatomies in the unitary domain, the definition of the anatomical landmarks to be set as interior boundary conditions plays a central role. Further analysis in this direction will be carried out. But the simplicity of the method and its robust mathematical background makes it a promising way to obtain a normalized anatomical space. On the other hand, other unitary domains, different from the unitary cube should be studied, in order to allow a clear definition of the apex central point and to take into account the right ventricle, specially the junction between its free wall and the septum.

References

1. Carapella, V., Bordas, R., Pathmanathan, P., et al.: Quantitative study of the effect of tissue microstructure on contraction in a computational model of rat left ventricle. PloS One **9**(4), e92792 (2014)
2. Casero, R., Burton, R.A.B., Quinn, T.A., Bollensdorff, C., Hales, P., Schneider, J.E., Kohl, P., Grau, V.: Towards high-resolution cardiac atlases: ventricular anatomy descriptors for a standardized reference frame. In: Camara, O., Pop, M., Rhode, K., Sermesant, M., Smith, N., Young, A. (eds.) STACOM 2010. LNCS, vol. 6364, pp. 75–84. Springer, Heidelberg (2010). doi:10.1007/978-3-642-15835-3_8
3. Desbrun, M., Meyer, M., Alliez, P.: Intrinsic parameterizations of surface meshes. Comput. Graph. Forum **21**, 209–218 (2002)
4. Evans, L.C.: Partial Differential Equations. American Mathematical Society, Providence (1998)
5. Garcia-Barnes, J., Gil, D., Badiella, L., et al.: A normalized framework for the design of feature spaces assessing the left ventricular function. TMI **29**(3), 733–745 (2010)
6. Gil, D., et al.: What a difference in biomechanics cardiac fiber makes. In: Camara, O., Mansi, T., Pop, M., Rhode, K., Sermesant, M., Young, A. (eds.) STACOM 2012. LNCS, vol. 7746, pp. 253–260. Springer, Heidelberg (2013). doi:10.1007/978-3-642-36961-2_29
7. Glocker, B., Sotiras, A., Komodakis, N., Paragios, N.: Deformable medical image registration: setting the state of the art with discrete methods*. Ann. Rev. Biomed. Eng. **13**, 219–244 (2011)
8. Gurgui, A., Gil, D., Marti, E.: Laplacian unitary domain for texture morphing. In: VISAPP (2015)
9. Helm, P., Beg, M.F., Miller, M.I., et al.: Measuring and mapping cardiac fiber and laminar architecture using diffusion tensor MR imaging. Ann. N. Y. Acad. Sci. **1047**, 296–307 (2005)
10. Karim, R., et al.: Surface flattening of the human left atrium and proof-of-concept clinical applications. Comput. Med. Imag. Graph **38**, 251–266 (2014)
11. Lamata, P., Niederer, S., Nordsletten, D., et al.: An accurate, fast and robust method to generate patient-specific cubic hermite meshes. Med. Image Anal. **15**(6), 801–813 (2011)
12. Lombaert, H., Grady, L., Pennec, X., Ayache, N., Cheriet, F.: Spectral log-demons: diffeomorphic image registration with very large deformations. IJCV **107**(3), 254–271 (2014)
13. Medrano-Gracia, P., Cowan, B.R., Suinesiaputra, A., et al.: Atlas-based anatomical modeling and analysis of heart disease. Drug Disc. Today Dis. Models **14**, 33–39 (2015)
14. Paun, B., Bijnens, B., Butakoff, C.: Subject independent reference frame for the left ventricular detailed cardiac anatomy. In: van Assen, H., Bovendeerd, P., Delhaas, T. (eds.) FIMH 2015. LNCS, vol. 9126, pp. 240–247. Springer, Heidelberg (2015). doi:10.1007/978-3-319-20309-6_28
15. Poveda, F., Marti, E., Andaluz, A., et al.: Helical structure of the cardiac ventricular anatomy assessed by diffusion tensor magnetic resonance imaging multiresolution tractography. Revista Española de Cardiología **66**(10), 782–790 (2013)
16. Soto-Iglesias, D., Butakoff, C., Andreu, D., et al.: Integration of electro-anatomical and imaging data of the left ventricle: an evaluation framework. Med. Image Anal. **32**, 131–144 (2016)

17. Vera, S., Ballester, M.A.G., Gil, D.: Anatomical parameterization for volumetric meshing of the liver. In: SPIE (2014)
18. Vera, S., González, M.A., Linguraru, M.G., Gil, D.: Optimal medial surface generation for anatomical volume representations. In: Yoshida, H., Hawkes, D., Vannier, M.W. (eds.) ABD-MICCAI 2012. LNCS, vol. 7601, pp. 265–273. Springer, Heidelberg (2012). doi:10.1007/978-3-642-33612-6_28
19. Young, A.A., Frangi, A.F.: Computational cardiac atlases: from patient to population and back. Exp. Physiol. **94**, 578–596 (2009)